

PACS numbers: 42.55.Rz; 42.60.Lh
DOI: 10.1070/QE2006v036n01ABEH013101

New laser transition in a Pr^{3+} : $RbPb_2Cl_5$ crystal in the 2.3 – 2.5-μm range

A.G. Okhrimchuk , L.N. Butvina, E.M. Dianov, N.V. Lichkova, V.N. Zagorodnev, A.V. Shestakov

***Abstract*. Lasing at the $^3F_3 - {}^3H_5$ transition of the Pr^{3+} ion in a nonhygroscopic Pr^{3+} : $RbPb_2Cl_5$ crystal is obtained for the first time at room temperature and the luminescent and lasing properties of the crystal are studied. The maximum differential cross section for stimulated emission in the 2.31 – 2.59-μm band of the $^3F_3 - {}^3H_5$ transition is found to be 1.7×10^{-19} cm^2 and the lifetime of the $^3F_3$ upper laser level is 0.11 ms.**

Keywords: *rare-earth ions, solid-state IR laser, phonon spectrum.*

1. Introduction

The use of optical technologies to control the environment pollution, for clinical diagnostics and solution of the problems of antiterrorism and other problems, which are based on the vibrational spectroscopy of chemical compounds, requires the development of reliable and comparatively low-cost light sources emitting in the mid-IR range with a low divergence. Solid-state lasers emitting at the electronic transitions of rare-earth ions satisfy these requirements. To fabricate such lasers, crystal matrices with a narrow phonon spectrum are needed. Crystals of the family $MePb_2Hal_5$, where Me = K or Rb and Hal = Cl or Br are promising for this purpose [1 – 3]. These crystals are not hygroscopic, unlike other chloride and bromide crystals. The Pr^{3+} ion is promising for lasing in the mid-IR range because it has a number of identically spin-degenerate levels in the energy region up to 7000 cm^{-1} and large oscillator strengths for transitions from the $^3F_3$ state to low-lying H states with the different orbital symmetry. Indeed, lasing at 5.2 and 7 μm at the $^3F_3 - {}^3F_2$ and $^3F_3 - {}^3H_6$ transitions in a $LaCl_3$ crystal was already demonstrated in papers [4, 5]. Unfortunately, this crystal has a serious disadvantage of being hygroscopic, which prevents its practical application as an active medium. We reported earlier the observation of lasing in a non-hygroscopic Pr^{3+} : $RbPb_2Cl_5$ crystal (Pr^{3+} : RPC) [6]. In this paper, we studied lasing in this crystal in more detail.

A.G. Okhrimchuk , L.N. Butvina, E.M. Dianov Fiber Optics Research Center, A.M. Prokhorov General Physics Institute, Russian Academy of Sciences, ul. Vavilova 38, 119991 Moscow, Russia;
e-mail: okhrim@fo.gpi.ru;
N.V. Lichkova, V.N. Zagorodnev Institute of Problems of Microelectronics Technology and High-purity Materials, Russian Academy of Sciences, 142432 Chernogolovka, Moscow region, Russia;
e-mail: lichkova@ipmt-hpm.ac.ru, zagorodnev@ipmr-hpm.ac.ru;
A.V. Shestakov Elements of Laser Systems Corporation, ul. Vvedenskogo 3, 117342 Moscow, Russia;
e-mail: avshest@rol.ru

Received 7 November 2005
Kvantovaya Elektronika **36** (1) 41 – 44 (2006)
Translated by M.N. Sapozhnikov

2. Sample fabrication

A Pr^{3+} : RPC crystal of diameter 8 mm was grown by the vertical Stockbarger – Bridgman method in a quartz ampoule. The initial material for the crystal growth was subjected to zone purification. The mass concentration of the $PrCl_3$ impurity in the charge was 1.0 %. A cylindrical active element made of the grown crystal had a length of 8 mm and a diameter equal to that of the crystal. The ends of the active element were perpendicular to the growth direction and their mutual non-parallelism did not exceed 30″. The active element was not coloured and did not contain any visible inclusions or bubbles, but its refractive index was slightly inhomogeneous over the element volume. The concentration of Pr^{3+} ions in the crystal measured with a mass spectrometer with an inductively coupled plasma was 0.27×10^{20} cm^{-3}, which corresponds to the mass concentration of $PrCl_3$ of 0.27 %. The crystal symmetry belongs to the monoclinic syngony (the spatial symmetry group $P2_1/c$). The parameters of the unit cell were $\alpha = 90^\circ$, $\beta = 90.1^\circ$, $a = 0.89$ nm, $b = 0.80$ nm, $c = 1.24$ nm [2]. Therefore, the crystal should be biaxial and its spectroscopic properties should depend on the polarisation direction.

3. Spectroscopic studies

Figure 1 shows the IR absorption spectra of the crystal for polarised light propagating along the growth axis. The spectra were recorded with a Vector-22 Bruker FTIR spectrometer with a resolution of 4 cm^{-1}. Polarisation directions correspond to the directions of minimal depolarisation of linearly polarised radiation of a 0.63-μm He – Ne laser. The polarisation properties of a Pr^{3+} : RPC crystal will be studied in detail separately.

The IR absorption spectrum exhibits two intense absorption bands at 1.56 and 1.98 μm. We assume that these bands are caused by transitions from the Stark sublevels of the ground state to the $^3F_3$ and $^3F_4$ multiplets (the 1.56-μm band) and the $^3F_2$ and $^3H_6$ multiplets (the 1.98-μm band). Figure 2 shows the low-energy part of the energy level diagram of the Pr^{3+} ion. The energy levels correspond to the maxima of the absorption bands.

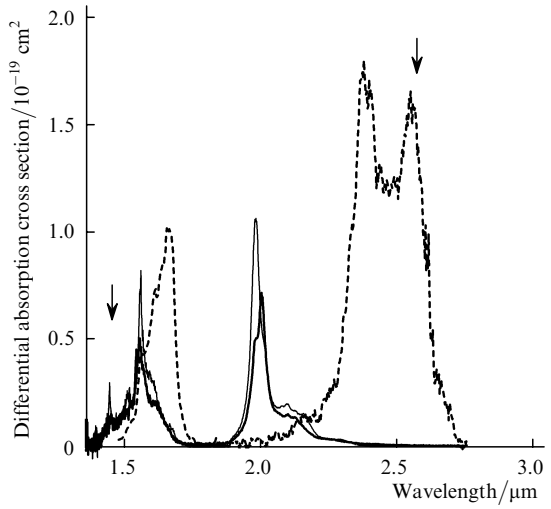

Figure 1. Differential cross section spectrum for stimulated transitions from the $^3F_3$ level [dashed curve calculated by (1)] and polarised spectra of the differential ground-state absorption cross section (solid curves). The arrows show the pump (1.45 μm) and laser (2.57 μm) wavelengths. The spectral resolution is 0.010 μm.

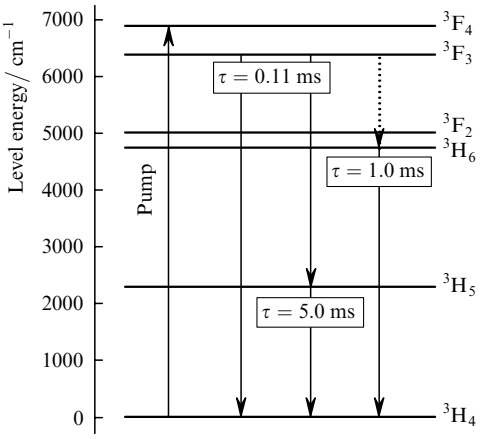

Figure 2. Diagram of the lower energy levels of the Pr^{3+} ion in the RPC crystal. The solid arrows are pump and luminescence transitions; the dotted arrow is the assumed luminescence transition; τ is the state lifetime.

We studied the luminescence and lasing properties of the crystal by pumping it by a Cr^{4+} : YAG laser at 1.45 μm. The pump laser consisted of a water-cooled $\varnothing 5 \times 50$-mm cylindrical active element, a plane highly reflecting mirror, and the output mirror with the radius of curvature 300 mm. The active element of the Cr^{4+} : YAG laser was pumped by linearly polarised radiation from a flashlamp-pumped Nd^{3+} : YAG laser through a dichroic highly reflecting mirror. The duration of the output pulse of the Cr^{4+} : YAG laser was 100 μs at the 0.1-maxium level and the pulse repetition rate was 2.5 Hz. The Cr^{4+} : YAG laser radiation was linearly polarised.

The luminescence spectra were recorded with a diffraction monochromator with a focal distance of 0.6 m. Luminescence in the range from 1.4 to 4 μm was detected with a PbS photoresistor and in the range from 4 to 6 μm – with a liquid-nitrogen-cooled MCT photoresistor. The search for and study of luminescence at longer wavelengths were restricted by absorption of the atmospheric water vapour. We found that the integrated luminescence kinetics observed after the end of the excitation pulse can be represented by the sum of three exponentials with the decay times 0.11, 1.0, and 5.0 ms. The time-resolved spectroscopy revealed four luminescence bands. The characteristics of the luminescence bands are presented in Table 1.

Table 1. Characteristics of luminescence transitions in the Pr^{3+} : RPC crystal at room temperature upon excitation of the $^3F_3 - {}^3F_4$ multiplets.

Transition	Wavelength range/μm	Luminescence decay time τ/ms	Band intensity
$^3F_3 - {}^3H_4$	1.55 – 1.69	0.11	strong
$^3F_3 - {}^3H_5$	2.31 – 2.59		strong
$^3F_2, {}^3H_6 - {}^3H_4$	1.96 – 2.55	1.0	weak
$^3H_5 - {}^3H_4$	4.0 – 5.1	5.0	weak

The analysis of the kinetic and luminescence spectra gives the following picture of the relaxation dynamics of Pr^{3+} ions. The Pr^{3+} ions pumped at 1.45 μm are excited from the ground state to the $^3F_4$ state and then undergo the rapid nonradiative transition to the close $^3F_3$ state (lying 500-cm^{-1} below the $^3F_4$ state) with the relaxation time shorter than 0.1 ms. The $^3F_3$ state is the initial state for radiative transitions to the $^3H_4$ and $^3H_5$ states corresponding to the 1.55 – 1.69-μm and 2.31 – 2.59-μm bands, respectively. The long-lived 4.0 – 5.1-μm luminescence band belongs to the following $^3H_5 - {}^3H_4$ transition. According to the energy level diagram in Fig. 2, the 1.96 – 2.55-μm luminescence band is related to the transitions from thermalised $^3F_2$ and $^3H_6$ multiplets to the $^3H_4$ ground state.

We assume that the $^3F_2$ and $^3H_6$ multiplets are mainly populated due to radiative transitions from the $^3F_3$ state. This conclusion is based on the estimate of the rate of multiphoton nonradiative relaxation of the $^3F_3$ state from the energy-gap law. The values of phenomenological parameters were taken from the study of relaxation of the excited states of Nd^{3+} ions in a related KPb_2Cl_5 crystal [7]. The calculated probability equal to 10^2 s^{-1} proved to be two orders of magnitude lower than the total decay probability of this state measured from the luminescence kinetics. Thus, we assume that the lifetime of the $^3F_3$ state is mainly determined by radiative transitions. We also found that the intensity of the 1.96 – 2.55-μm luminescence band belonging to the $^3F_2$, $^3H_6 - {}^3H_4$ transition was an order of magnitude lower than the intensity of luminescence from the $^3F_3$ state. This means that the branching ratio of luminescence for the $^3F_3 - {}^3F_2$ and $^3F_3 - {}^3H_6$ transitions is small, which complicates the search for luminescence beginning from the $^3F_3$ level in the 5 – 8-μm region (the dotted arrow in Fig. 2).

We constructed the spectrum of differential cross section for stimulated transitions by the method proposed by McCumber [8]. A simplified model was considered in which the angular luminescence intensity distribution for each Pr^{3+} ion corresponded to radiation of three identical mutually orthogonal dipoles. After simple transformations of formulas from [8], we obtain the expression

$$\sigma_{em}(\lambda) = \frac{A_{em}\lambda^4}{8\pi c n^2} \frac{F(\lambda)}{\int_0^\infty F(\lambda)\mathrm{d}\lambda}, \quad (1)$$

which can be considered as the generalisation of the Fechtbauer – Ladenburg formula, where $F(\lambda)$ is the lumi-

nescence spectrum in photons per second within the unit wavelength interval, determined with an accuracy to a constant; A_{em} is the total emission probability of a photon from the given state; $n \approx 2$ is the refractive index; and c is the speed of light in vacuum. According to the above discussion, $A_{em} = 1/\tau = 0.99 \times 10^4$ s^{-1}. Figure 1 shows the spectrum of the differential cross section for stimulated transitions from the $^3F_3$ state plotted by expression (1).

4. Lasing experiments

We studied lasing by focusing pump radiation with a lens with a focal distance of 15 cm into a spot of diameter $d =$ 450 μm on the active element. In this case, orange emission was observed in the pumped region. This emission was not observed when the crystal was pumped by a laser beam with a greater diameter ($d > 2$ mm) and the same pulse energy. These facts suggest that up-conversion processes exist which can deplete the population at the upper $^3F_3$ laser level. The resonator for the wavelength range 2.30–2.65 μm was formed by a highly reflecting meniscus mirror with the radius of curvature 15 cm and a plane output mirror. The active element was located near the output mirror. It was pumped through the highly reflecting mirror with the transmission coefficient $T = 0.6$ % in the 2.2–2.7-μm region and 70 % at the pump wavelength.

The orientation of the active element was optimised by rotating it around the optical axis so that the direction of the pump polarisation would correspond to the maximum absorption of pump radiation (the absorption spectrum for this case is shown by a thin solid curve in Fig. 1). Because the crystal had no AR coatings, its axis was made precisely coincident with the optical axis of the resonator to minimise the Fresnel losses of radiation reflected from the crystal faces. Lasing was obtained on the long-wavelength tail of the emission band by using nonselective output mirrors with the transmission coefficients $T = 1.2$ % and 2.5 % in the wavelength range 2.31–2.59 μm. The laser pulse appeared at the instant of the pump pulse maximum and was shorter than the latter by 30 %. The laser wavelength with the output mirror with $T = 1.2$ % was 2.57 μm.

The resonator length was set equal to 1.8 cm to provide the maximum conversion efficiency of the pump radiation. Figure 3 shows the dependence of the laser pulse energy on the absorbed pump pulse energy for such a resonator. The maximum efficiency of 1.6 % was achieved with the output mirror with $T = 2.5$ %. The threshold pump energies determined from the energy dependences presented in the insert in Fig. 3 were 1.01 ± 0.05 mJ and 1.24 ± 0.05 mJ for mirrors with $T = 1.2$ % and 2.5 %, respectively. These data allow us to estimate the intracavity losses by the Findlay–Clay method [9]. According to this method, the threshold pump energy linearly depends on the logarithmic losses ξ at the input mirror:

$$E_{th}(\xi) = E_0\left(1 + \frac{\xi}{L}\right), \qquad (2)$$

where L are the round-trip intracavity losses and E_0 is the threshold pump energy for a cavity with the highly reflecting mirrors. The solution of a system of two equations (2) written for two output mirrors gives the intracavity losses (including the output losses for the highly reflecting mirror). A great error in the determination of the threshold energy causes a great error in the estimate of intracavity losses. The intracavity losses were calculated to be in the range from 35 % to 10 %.

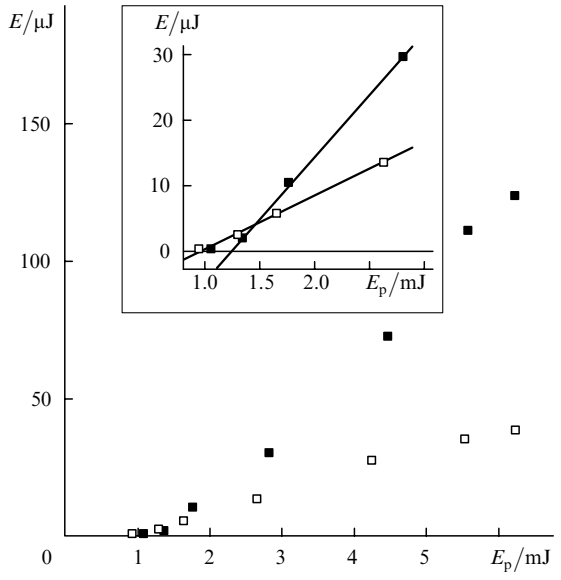

Figure 3. Dependences of the output pulse energy E on the absorbed pump pulse energy E_p. Squares are the experimental results obtained for the output mirror transmission $T = 2.5$ % (■) and 1.2 % (□). The insert shows the dependences in more detail near the lasing threshold; the solid curves are the linear approximations of the experimental data made to determine the threshold pump energy.

5. Discussion of experiments

Considerable intracavity losses are caused by the absence of AR coatings on the ends of the active element and the bad optical quality of the crystal. The latter circumstance was the indirect reason of a poor matching of the laser mode with the pumped volume of the crystal. For the separation of the resonator mirrors equal to 1.8 cm, the calculated diameter of the fundamental mode in the active element was 270 μm, which is considerably smaller than the pump spot diameter $d = 450$ μm. We attempted to increase the mode diameter by increasing the distance between resonator mirrors, but this reduced the efficiency due to the dominating increase in the intracavity losses caused by the inhomogeneity of the refractive index in the crystal volume. Thus, it seems that high intracavity losses are the main reason for the low conversion efficiency of the pump radiation energy to the output pulse energy. The depletion of the upper laser level due to up-conversion can also reduce the conversion efficiency; however, to determine the contribution of up-conversion, additional investigations are required.

We assume that the shift of the laser wavelength with respect to the wavelength corresponding to the maximum of the stimulated-transition cross section is caused by the distortion of the gain profile due to absorption at the $^3H_4 - {}^3H_6$ transition. However, the latter transition does not prevent in principle lasing in the $^3F_3 - {}^3H_5$ transition band. We assume that the laser can be tuned within the 2.31–2.59-μm band by using the adequate pump energy.

6. Conclusions

We have grown the Pr^{3+} : $RbPb_2Cl_5$ crystals of the optical quality with a high concentration of Pr^{3+} ions. The spectrum of the differential cross section for stimulated transitions from the $^3F_3$ state has been determined. We have found that the stimulated $^3F_3 - {}^3H_5$ transition has a greater cross section in the 2.31 – 2.59-μm emission band and obtained lasing at this transition. Because the lifetime of the upper laser level is quite long, this new crystal can be efficiently used in *Q*-switched mid-IR lasers.

Acknowledgements. The authors thank A.M. Onischenko for discussion of the results of this paper.

References

1. Nostrand M.C., Page R.H., Payne S.A., Isaenko L.I., Yelisseyev A.P. *J. Opt. Soc. Am. B*, **18** (3), 264 (2001).
2. Nitsch K., Dusek M., Nikl M., Polak K., Rodova M. *Prog. Crystal Growth and Charact.*, **30**, 1 (1995).
3. Rademaker K., Heumann E., Huber G., Payne S.A., Krupke W.F., Isaenko L.I., Burger A. *Opt. Lett.*, **30** (7), 729 (2005).
4. Bowman S.R., Ganem J., Feldman B.J., Kueny A.W. *IEEE J. Quantum Electron.*, **30**, 2925 (1994).
5. Bowman S.R., Shaw L.B., Feldman B.J., Ganem J. *IEEE J. Quantum Electron.*, **32**, 646 (1996).
6. Okhrimchuk A., Butvina L., Dianov E., Lichkova N., Zavgorodnev V., Shestakov A. *Proc. Int. Conf. on Lasers, Applications and Technologies (LAT)* (St. Petersburg, Russia, 2005) LThG3.
7. Tkachuk A.M., Ivanova S.E., Isaenko L.I., Eliseev A.P., Payne S., Solarz R., Page R., Nostrand M. *Opt. Spektr.*, **92**, 89 (2002).
8. McCumber D.E. *Phys. Rev.*, **134**, A299 (1964).
9. Findlay D., Clay R.A. *Phys. Lett.*, **20**, 277 (1966).